Eur. Phys. J. A **13**, 9–14 (2002)

**THE EUROPEAN PHYSICAL JOURNAL A**



# Nuclear structure in the vicinity of the N = Z line in the A = 90–100 region

A. Johnson[1,a]

[1] Department of Physics, Royal Institute of Technology, S-104 05 Stockholm, Sweden
[2] Chemistry Department, Washington University, St. Louis, MO 63130, USA
[3] Nuclear Science Division, Lawrence Berkeley Laboratory, Berkeley, CA 94720, USA
[4] Department of Physics, Lund University, Lund, Sweden
[5] Department of Neutron Research, Uppsala University, Uppsala, Sweden
[6] Chalmers University of Technology, Gothenburg, Sweden
[7] Physikalisches Institut, University of Göttingen, Göttingen, Germany
[8] Laboratori Nazionali di Legnaro, INFN, Italy
[9] Argonne National Laboratory, Argonne, IL 60439, USA
[10] Institute of Theoretical Physics, Warsaw University, Warsaw, Poland
[11] H. Hulubei National Institute for Physics and Nuclear Engineering, Bucharest, Romania
[12] Dipartimento di Fisica dell'Università and INFN, Sezione di Padova, Italy
[13] Instituto de Física Corpuscular, Valentia, Spain
[14] Dipartimento di Chimica Fisica dell'Università di Venezia and INFN, Sezione di Padova, Italy
[15] Grupo de Física Nuclear, Universidad de Salamanca, Spain
[16] Heavy Ion Laboratory, University of Warsaw, Warsaw, Poland
[17] Institute for Nuclear Research, Debrecen, Hungary
[18] Department of Physics, Helsinki University, Helsinki, Finland
[19] GSI, Darmstadt, Germany
[20] Niels Bohr Institute, University of Copenhagen, Copenhagen, Denmark
[21] J. Stefan Institute, Ljubljana, Slovenia
[22] Soltan Institute for Nuclear Studies, Swierk, Poland

Received: 1 May 2001

**Abstract.** Neutron-deficient nuclei in the mass region $A \approx 90$–$100$ exhibit a large variety of phenomena. In this region the heaviest $N = Z$ nuclei are identified and enhanced neutron-proton correlations are expected when protons and neutrons occupy identical orbitals. A variety of nuclear shapes are predicted and observed for $A \leq 91$, including superdeformed shapes. The nucleus $^{100}$Sn is the heaviest $N = Z$ doubly magic nucleus believed to be bound. Knowledge of the shell structure around $^{100}$Sn is of utmost importance for understanding the nuclear shell model. New results on both the $N = Z$ nucleus $^{88}$Ru, superdeformed structures in $A \approx 90$ nuclei as well as the first result on the level structure in $^{103}$Sn, and an extended level structure in $^{102}$In are presented. The limitations of using stable beams and targets and the possibilities with new radioactive beams are briefly outlined.

**PACS.** 21.10.Re Collective levels – 21.60.Cs Shell model – 27.50.+e $59 \leq A \leq 89$ – 27.60.+j $90 \leq A \leq 149$

## 1 Introduction

The $A \approx 90$–$100$ mass region has attracted large attention during recent years. A variety of phenomena are predicted in nuclei far off stability and close to or at the $N = Z$ line in this region. Nuclei with $N \approx Z$ are believed to show enhanced neutron-proton correlations when neutrons and protons occupy identical orbitals. The manifestation and signatures of such correlations are still under debate. New theoretical attempts are being made to try to disentangle the effects of enhanced neutron-proton correlations on, *e.g.*, masses, excitation energies, moments of inertia and crossing frequencies. Of special interest is the nucleus $^{100}$Sn which is the heaviest doubly magic self-conjugate ($N = Z$) nucleus believed to be bound. Information on the structure of nuclei close to $^{100}$Sn is of utmost importance for studying residual interactions and single-particle energies and testing the validity of the nuclear shell model in this region. In addition these nuclei are located close to

[a] In collaboration with groups 1-22.

the proton drip line implying that coupling to continuum states may influence the nuclear structure.

New highly effective arrays for $\gamma$-ray spectroscopy like EUROBALL [1] and GAMMASPHERE [2] , combined with state-of-the-art ancillary detectors and/or recoil mass separators, have allowed identification and in-beam $\gamma$-spectroscopic studies in heavy-ion–induced fusion evaporation reactions of very neutron-deficient nuclei close to the $N = Z$-line in this mass region. So far the results have been obtained with stable beams and targets. The access to radioactive beams with sufficient intensities are believed to allow investigations of even more exotic nuclei in this mass region.

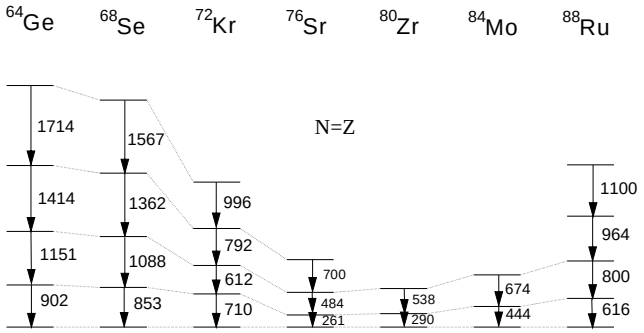


**Fig. 2.** Yrast states in even-even $N = Z$ nuclei. The transition energies are given in keV.

## 2 N = Z nuclei

Until now, the heaviest doubly even $N = Z$ nucleus with known excited levels has been $^{84}$Mo in which the $2^+$ and $4^+$ states are known [3,4]. In a new experiment at GASP, Legnaro, excited states in the $N = Z = 44$ nucleus $^{88}$Ru have been observed for the first time [5]. A 105 MeV beam of $^{32}$S from the Legnaro Tandem accelerator was used to initiate fusion reactions on a 1.1 mg/cm$^2$ target of $^{58}$Ni evaporated on a Au backing. The $\gamma$-rays were detected with the GASP array [6] with 40 Compton-suppressed HPGe detectors and an inner BGO ball. For reaction channel identification six NE213 neutron detectors and the ISIS $E$-$\Delta E$ silicon ball were used. The $\gamma$-rays following the 2n reaction channel leading to $^{88}$Ru were observed in a $\gamma$-$\gamma$ matrix sorted in coincidence with neutrons but in anticoincidence with charged particles in the ISIS ball. A summed coincidence spectrum obtained with gates on three $\gamma$-transitions attributed to $^{88}$Ru is shown in fig. 1. The estimated cross-section for producing $^{88}$Ru is 5–10 $\mu$b (For more details and references, see [5]).

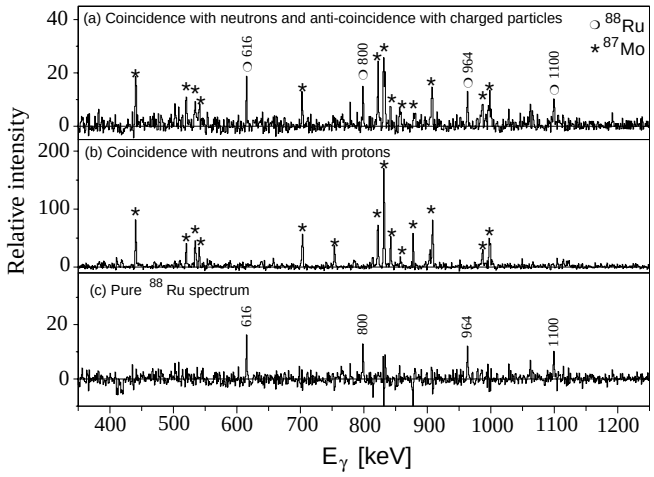


**Fig. 1.** Sum of gates on the 616, 800 and 964 keV $\gamma$-lines in $\gamma$-$\gamma$ matrices obtained in coincidence with neutrons and (a) in anticoincidence with charged particles, (b) in coincidence with protons. Spectrum (c) shows the difference between the two upper spectra taking into account the measured proton efficiency.

Looking at the systematics of the yrast levels in $N = Z$ nuclei from $^{64}$Ge to $^{88}$Ru, fig. 2, one observes a decrease in the energy of the $2^+$ state with increasing mass number up to $^{76}$Sr indicating a more collective behaviour and a deformed structure. At $^{80}$Zr this tendency changes and the excitation energy of the $2^+$ state increases again when moving towards the predicted spherical shape of $^{100}$Sn. Also the ratio of $E^{4+}$ to $E^{2+}$ reaches a maximum of about 2.85 at $^{76}$Sr and $^{80}$Zr indicating a rotational-like structure. The new results on $^{88}$Ru with $E^{2+} = 616$ keV and an $E^{4+}$ to $E^{2+}$ ratio of 2.3, follow the observed tendency and indicate a transitional structure of this nucleus. The theoretical predictions of the ground-state deformation in $^{88}$Ru vary from oblate to almost spherical to weakly prolate deformed ($\varepsilon_2 = 0.1$–$0.2$). A determination of the size and the sign of the quadrupole moment of $^{88}$Ru would be of great value for testing the various theoretical approaches, especially those which take into account different types of pairing interactions (see [5]).

In $^{72}$Kr [7,8] a shape change is inferred at low excitations. In this nucleus, as well as in $^{80}$Zr [8] , which both have been studied to high rotational frequencies, a delay in the aligment of $g_{9/2}$ protons/neutrons is observed as compared to standard TRS calculations. In $^{88}$Ru no indication of a backbend is observed up to a rotational frequency of 0.55 MeV. A delay in alignment frequency has been suggested to be a signature of $T = 0$ neutron-proton pairing correlations or a coupling to vibrational degrees of freedom [7]. $T = 0$ neutron-proton pairs coupled to $J_{\max}$ will successively align with rotation whereas n-p pairs coupled to $J = 1$ will break up with rotation like nn- and pp-pairs but at a higher rotational frequency if $G_{T=0} > G_{T=1}$. Here the importance of the various $J$-values will determine the all over behaviour [9].

Other possible signatures of $T = 0$ neutron-proton pairing have been discussed by many authors. Recently Satula and Wyss [10] have demonstrated that the $T = 0$ pairing field can give a microscopic explanation of the Wigner energy in even-even $N = Z$ nuclei. The same authors have also studied in TRS calculations the influence of $T = 0$ pairing interactions on the dynamical moment of inertia of the predicted superdeformed band in $^{88}$Ru [9]. In fig. 3 calculations without pairing, with only standard $T = 1$ pairing and with the inclusion also of $T = 0$ pair-

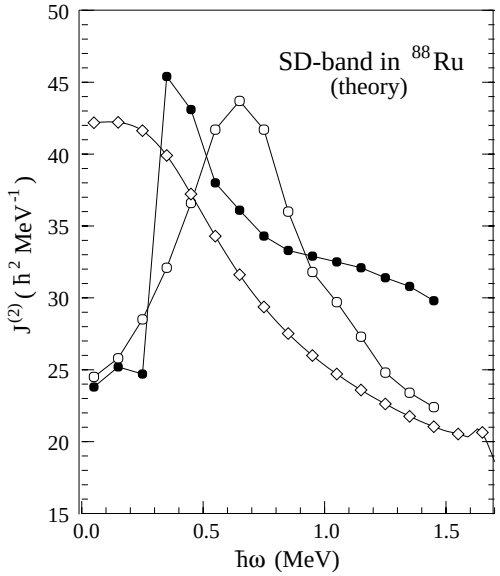


**Fig. 3.** Theoretical dynamical moments of inertia $\mathcal{J}^{(2)}$ for the SD band in $^{88}$Ru. The different curves show calculations with no pairing ($\diamond$), with standard $T = 1$ pairing ($\circ$) and with the inclusion of also $T = 0$, $\alpha$-$\alpha$ pairing ($\bullet$). The sharp rise at 0.3 MeV is due to a pairing phase transition from $T = 1$ to $T = 0$.

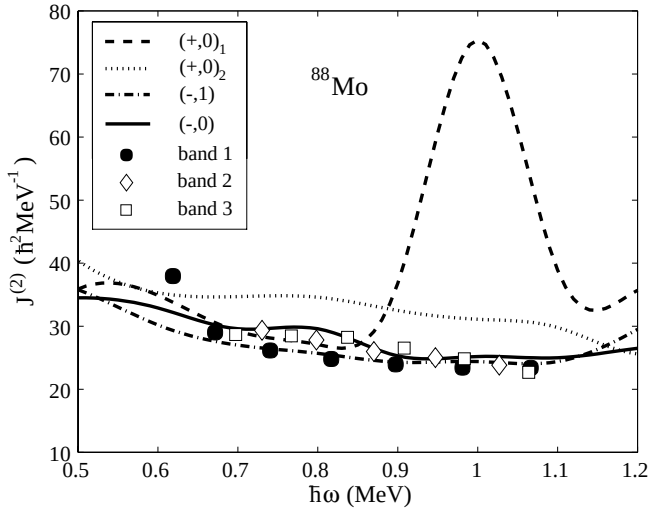


**Fig. 4.** Experimental dynamical moments of inertia $\mathcal{J}^{(2)}$ (symbols) for the three SD bands in $^{88}$Mo compared to values from a cranked Strutinsky calculation (lines). The experimental data correspond better to the $(\pi, \alpha) = (-, 1)$ and $(-, 0)$ (proton excitation) configurations (both with $\beta_2 \approx 0.5$) than to the two vacuum configurations $(+, 0)_1$ ($\beta_2 \approx 0.5$) and $(+, 0)_2$ ($\beta_2 \approx 0.65$).

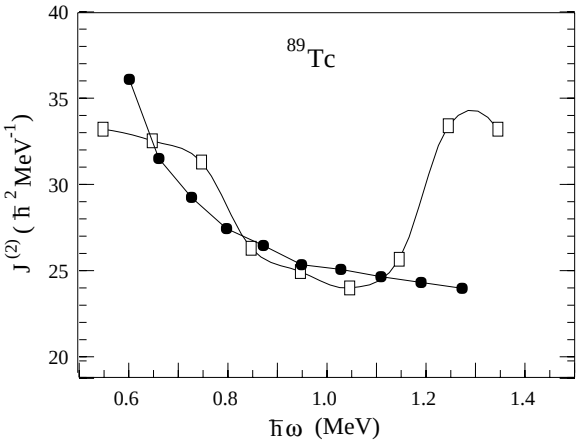


**Fig. 5.** Experimental (filled circles) and theoretical (open squares) dynamical moments of inertia $\mathcal{J}^{(2)}$ for the SD band in $^{89}$Tc.

ing are shown. Note especially the different behaviours at high rotational frequencies. Thus the behaviour of the dynamical moment of inertia in a SD band may also serve as an indicator of $T = 0$ pairing.

A further signature may be the excitation energy of $T = 2$, $I = 0$ states in even-even $N = Z$ nuclei. In studies of isobaric analogue states in $N = Z$ nuclei by means of rotations in isospace, Satula and Wyss [11] have obtained excellent agreement for the energies of the lowest excited $I = 0$, $T = 2$ states in $20 < A < 56$ nuclei when including both $T = 0$ and $T = 1$ pairing. Calculations with only $T = 1$ pairing are about a factor of two off.

## 3 Superdeformed structures in A ≈ 90 nuclei

The $A = 80$–$90$ region was early predicted to be favoured for observation of superdeformed (SD) structures and a number of SD bands have now been reported for nuclei with $A = 80$–$91$. Large energy gaps at SD shapes for especially $N = Z = 38, 42, 44, 46$ stabilize these structures. Theoretically the nucleus $^{88}$Ru, already presented above, is predicted to have a "doubly magic" SD structure with two protons and two neutrons in the lowest $N = 5$ intruder orbitals (denoted as a $\pi 5^2, \nu 5^2$ configuration). With rotation the $N = Z = 42$ gap below the $N = 5$ orbitals gets quenched and a new gap opens up at nucleon number 43 with one particle in the $N = 5$ orbital. In the early interpretations in *e.g.* [12], the SD structure in $^{83}$Sr was believed to involve a $\pi 5^1, \nu 5^3$ configuration. Subsequent lifetime measurements for SD bands in the $A \approx 80$ region [13] indicate deformations of $\beta_2 \approx 0.45$–$0.50$ for $^{80}$Sr-$^{83}$Sr but larger deformations ($\beta_2 \approx 0.55$) for $^{83}$Y and $^{84}$Zr. The deduced transition quadrupole moments are supported by new calculations in [13] indicating that the SD bands in the Sr-isotopes have $\pi 5^0, \nu 5^1$ configurations. In $^{83}$Y and $^{84}$Zr, on the other hand, $\pi 5^1, \nu 5^2$ structures are causing the larger deformations. Our calculations also show that it is possible to occupy a single $N = 5$ proton orbital only for $Z > 38$.

Recently SD structures have been reported for $^{88}$Mo [14], $^{89}$Tc [15] and $^{91}$Tc [16] which are the heaviest nuclei in this region with known SD structures. The structures in the first two nuclei are quite well reproduced in TRS calculations as seen in figs. 4 and 5 showing plots of experimental and theoretical dynamical moments of inertia $\mathcal{J}^{(2)}$. In $^{88}$Mo the observed SD structures are ex-

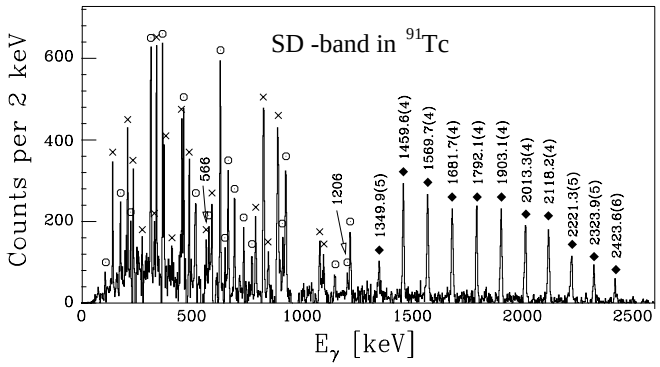


**Fig. 6.** Summed coincidence $\gamma$-ray spectrum obtained by double gating in the $1\alpha 3$p data on all transitions in the SD band (filled diamonds) in $^{91}$Tc. Transitions in previously known positive and negative structures that appear in coincidence with the new SD band are indicated by open circles and crosses, respectively.

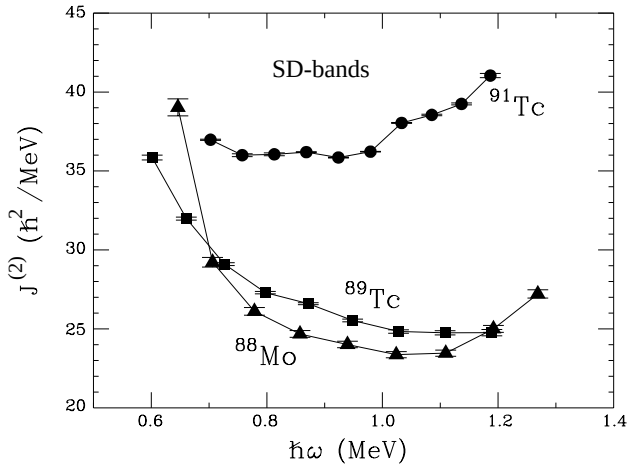


**Fig. 7.** Dynamical moments of inertia $\mathcal{J}^{(2)}$ *versus* rotational frequency of the SD bands in $^{88}$Mo, $^{89}$Tc and $^{91}$Tc.

plained as two-quasi-particle proton configurations with one proton excited to a $N = 5$ orbital rather than being built on the two vacuum configurations at $\beta_2 \approx 0.5$ and 0.65, respectively. Two neutrons occupy the $N = 5$ high-$j$ orbitals. In $^{89}$Tc the configuration $\pi 5^1, \nu 5^2$ gives a rather good fit to the experimental data as seen in fig. 5. The calculated increase in the $\mathcal{J}^{(2)}$ moment of inertia at high frequencies in fig. 5 is due to a change in deformation towards larger triaxiality and smaller $\beta_2$ and $\beta_4$ values.

In $^{91}$Tc a SD band has been observed in a GAMMASPHERE experiment [16]. Figure 6 shows a summed coincidence spectrum. The deduced transition quadrupole moment of $Q_t = 8.1^{+1.9}_{-1.4}$ $e$b for this SD band should be compared to $Q_t = 6.0^{+2.0}_{-1.4}$ $e$b and $Q_t = 6.7^{+3.0}_{-2.3}$ $e$b for the SD bands in $^{88}$M and $^{89}$Tc, respectively. By scaling observed quadrupole moments in various mass regions with $ZR^2$ [16], one finds that $^{91}$Tc shows values comparable to those in the $A \approx 150$ region and considerably larger than those deduced in other nuclei in the $A \approx 80$ region.

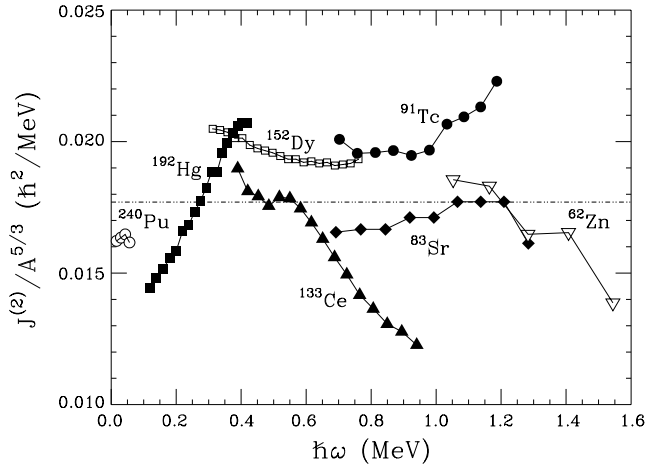


**Fig. 8.** Scaled dynamical moments of inertia ($\mathcal{J}^{(2)}/A^{\frac{5}{3}}$) *versus* rotational frequency of selected SD bands from various mass regions.

Also the $\mathcal{J}^{(2)}$ moment of inertia of the SD band in $^{91}$Tc shows quite a different behaviour as compared to those in $^{88}$Mo and $^{89}$Tc (fig. 7). Comparing scaled moments of inertia ($\mathcal{J}^{(2)}/A^{\frac{5}{3}}$) of SD bands from various mass regions (fig. 8), one finds that the SD band in $^{91}$Tc reaches the highest values together with $^{152}$Dy. Thus the SD band in $^{91}$Tc shows unique properties as compared to other SD bands in the $A = 80$–90 region and an addition of two extra neutrons to $^{89}$Tc radically changes the properties of the SD band.

Cranked Strutinsky calculations based on the Woods-Saxon potential have been performed to try to explain the structure of the SD band in $^{91}$Tc [16]. Pairing correlations were taken into account by means of a seniority and double stretched quadrupole pairing force [17] and approximate particle number projection was performed by means of the Lipkin-Nogami method [18,19]. Two different parametrisations of the Woods-Saxon potential have been used but no firm conclusions can be drawn about the detailed structure of the SD band in $^{91}$Tc. The $\pi 5^1, \nu 5^2$ configuration, giving a rather good explanation of the SD structure in $^{89}$Tc, is predicted to be the lowest in energy but fails to describe the $\mathcal{J}^{(2)}$ moment of inertia as obvious in fig. 9. The best agreement for part of the frequency range is obtained for the $\pi 5^2, \nu 5^4$ configuration with $\beta_2 \approx 0.7$, thus involving three additional $N = 5$ orbitals as compared to the SD band in $^{89}$Tc. This would imply one of the most deformed structures observed. More accurate lifetime measurements are needed to more firmly confirm this interpretation.

## 4 The $^{100}$Sn region

The first $^{100}$Sn nuclei were identified a few years ago. So far no excited states are known in $^{100}$Sn. The closest neighbours of $^{100}$Sn with known excited states are $^{98}$Cd [20] and $^{102}$Sn [21] with two proton-holes and two neutron particles, respectively, outside the doubly closed

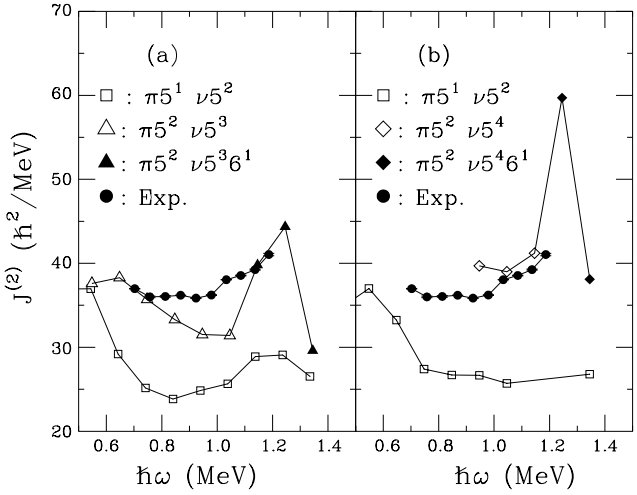


**Fig. 9.** Calculated and experimental $\mathcal{J}^{(2)}$ moments of inertia. The two calculations use different parametrisations of the Woods-Saxon potential.

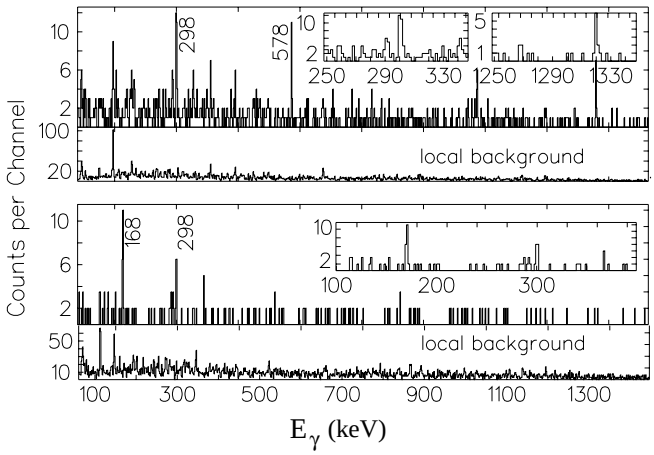


**Fig. 10.** $\gamma$-ray spectra obtained in coincidence with the 168 keV (upper spectrum) and 1318 keV (lower spectrum) transitions in $^{103}$Sn. Expanded parts are shown as inserts.

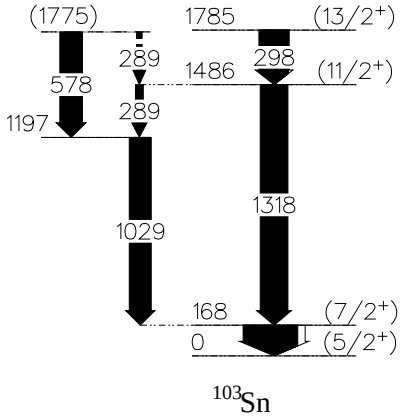


**Fig. 11.** Level scheme of $^{103}$Sn. The widths of the arrows indicate the $\gamma$-ray intensity.

core. Those nuclei were produced at NBI, Denmark, in heavy-ion fusion reactions with cross-sections of a few $\mu$b utilizing EUROBALL cluster detectors and NORDBALL ancillary detectors for channel selection. Gamma-rays following the decay of the isomeric ($\mu$s-range) $8^+$ and $6^+$ states in $^{98}$Cd and $^{102}$Sn, respectively, were recorded at a catcherfoil 60 cm downstreams the target. For $^{102}$Sn a complementary measurement of conversion electrons [22] at the FMA in Argonne, has revealed the previously unobserved 48 keV $6^+$-$4^+$ transition.

With the structure of the closest odd-$A$ neighbours of $^{100}$Sn still unknown, information on single-particle energies outside of $^{100}$Sn has relied on shell model calculations for more distant odd-$A$ nuclei with known structures. Those estimates are afflicted with large uncertainties. The second best estimate of neutron single-particle energies outside of $^{100}$Sn, after $^{101}$Sn, is provided by $^{103}$Sn. An experiment aimed at identifying the level structure in $^{103}$Sn [23] has therefore been performed at Legnaro, Italy, using the EUROBALL detector array equipped with 15 cluster detectors and 26 clover detectors and supplemented with the ISIS charged particle $E$-$\Delta E$ Si ball and a 50-element neutron wall covering $1\pi$ in the forward direction. A 1.4 mg/cm$^2$ $^{54}$Fe target, evaporated on an Au-backing, was bombarded with a beam of 240 MeV $^{58}$Ni ions. The $2\alpha$1n channel leading to $^{103}$Sn was identified by selecting $\alpha$-particles in the $E$-$\Delta E$ spectra and neutrons in time-of-flight (TOF) *versus* zero-cross-over (ZCO) time spectra. The estimated cross-section is $5 \pm 3\,\mu$b. Several candidates for $\gamma$-lines belonging to $^{103}$Sn were found. Despite low statistics, it was possible to establish coincidence relations between those candidates in a prompt $\gamma$-$\gamma$ coincidence matrix obtained with proper particle gates, fig. 10. For some transitions it was also possible to deduce information on angular distributions from intensity ratios obtained at different detectors angles. The level scheme constructed from these data is shown in fig. 11.

A new shell model calculation has been performed within the neutron single-particle basis $1g_{7/2}$, $2d_{5/2}$, $2d_{3/2}$, $3s_{1/2}$ and $1h_{11/2}$ with matrix elements from the Bonn $A$ potential. Some empirical corrections have been applied to obtain the best overall fit to $^{102\text{-}114}$Sn. The new data on $^{103}$Sn, with the $7/2^+$ state 168 keV above the $5/2^+$ ground state, gives further constraints on the single-particle energy difference $\epsilon 1g_{7/2} - \epsilon 2d_{5/2}$ which is an important result. The deduced value is $\epsilon 1g_{7/2} - \epsilon 2d_{5/2} = 0.11(4)$ MeV. In addition the single-particle energy differences $\epsilon 3s_{1/2} - \epsilon 2d_{5/2} = 1.6(2)$ MeV, $\epsilon 2d_{3/2} - \epsilon 2d_{5/2} = 2.0(2)$ MeV and $\epsilon 1h_{11/2} - \epsilon 2d_{5/2} = 2.3(2)$ MeV are obtained. The calculations give in general a good agreement with the experimental results with some exceptions. The spacing between the yrast $4^+$ and $2^+$ levels in $^{104}$Sn is underestimated with about 200 keV in the calculations which might be due to a coupling to core excitations across the $N = Z = 50$ gap. An identification of the $17/2^+$ and $15/2^+$ levels in $^{103}$Sn might shed light on this discrepancy.

The level schemes of several other final nuclei populated in the same experiment have been extended. In $^{102}$In, produced via the $2\alpha$1p1n reaction, the level structure was earlier established up to spin (11) [24] at about 2 MeV. In this experiment the level scheme has tentatively

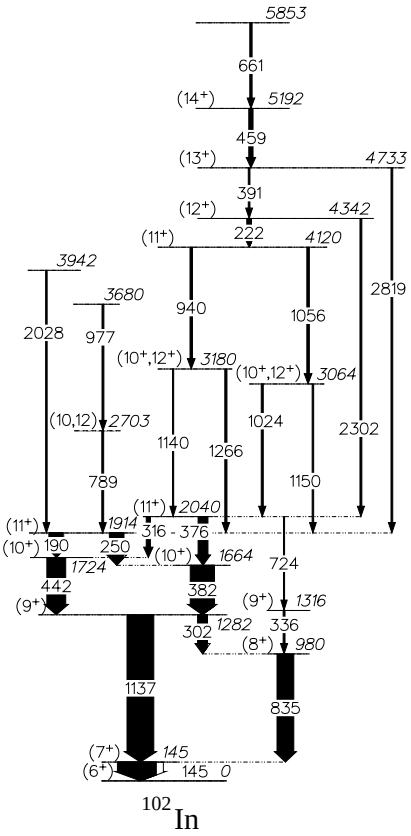


**Fig. 12.** Preliminary extended level scheme of $^{102}$In. The widths of the arrows indicate the $\gamma$-ray intensity.

been extended up to 5.85 MeV [25]. The preliminary level scheme is shown in fig. 12. The levels up to 2040 keV are reproduced with an accuracy better than 100 keV in the framework of a shell model calculation within the basis $\pi g_{9/2}^{-1}\nu(g_{7/2}, d_{5/2}, d_{3/2}, s_{1/2}, h_{11/2})^3$. A band-like structure consisting of low-energy $M1$ transitions was also observed above 4 MeV. One possible interpretation is that the $\nu g_{9/2}^{-1}\nu(d_{5/2}, g_{7/2})^{+1}$ core excitation is a main ingredient in the $(11^+)$ band head. The $\nu g_{9/2}^{-1}$ and $\pi g_{9/2}^{-1}$ holes can couple to a very stable $9^+$ hole structure. Coupling this structure to a fully aligned $\nu[g_{7/2}, d_{5/2}]^2_{6^+}$ particle state at $\approx 90^\circ$ for minimal energy, a spin of $\approx 11$ is obtained. Assuming such a configuration, it is possible from the excitation energies of the $M1$ band to deduce a measure of the $E(\nu d_{5/2}) - E(\nu g_{9/2})$ single-particle energy difference defined as the difference between the neutron separation energies of $^{100}$Sn and $^{101}$Sn. After some corrections taking into account various interactions, the $N = 50$ shell gap is estimated to be 4.6(5) MeV (see further [25]).

## 5 Summary and perspectives

New experimental techniques together with stable beams and targets have allowed investigations of the nuclear structure of many neutron-deficient nuclei in the $A =$ 90–100 region. Levels in even-even $N = Z$ nuclei up to $^{88}$Ru have been observed and we are approaching $^{100}$Sn. The limits using fusion evaporation reactions with stable beams and targets seem today to be set by reactions involving emission of up to two neutrons. That means that the heaviest even-even $N = Z$ nuclei that might be reached in this way are $^{92}$Pd and $^{96}$Cd. To reach even more neutron-deficient nuclei and especially get closer to $^{100}$Sn, we most probably need radioactive beams. Therefore, the access to radioactive beams that can bring us to $^{100}$Sn and its closest neighbours, as well as out to the proton drip line over a wide mass range, is of great importance for extending our knowledge in this region where such a richness of phenomena are expected. In the first step, beams of large interest for fusion evaporation reactions in the $A = 80$–$100$ region are, *e.g.*, $^{56}$Ni, $^{72,74}$Kr and $^{34}$Ar which are soon becoming available at RIB facilities. However, low beam intensities and very low relative cross-sections may still make such investigations very difficult.

In this overview results from several groups and colleagues are presented and the author likes to thank all the involved persons. Special thanks go to N. Mărginean *et al.* for the permission to show results on $^{88}$Ru prior to publication.

## References

1. J. Gerl, R.M. Lieder (Editors), *EUROBALL III, a European $\gamma$-ray Facility*, Technical Report (GSI, 1992).
2. I.-Y. Lee, Nucl. Phys. A **520**, 641c (1990).
3. W. Gelletly *et al.*, Phys. Lett. B **253**, 287 (1991).
4. D. Bucurescu *et al.*, Phys. Rev. C **56**, 2497 (1997).
5. N. Mărginean *et al.*, Phys. Rev. C **63**, 031303 (2001).
6. D. Bazzacco, in *Proceedings of the International Conference on Nuclear Structure at High Angular Momentum, Ottawa*, Vol. **II**, Report no. AECL-10613 (1992) p. 376.
7. G. de Angelis *et al.*, Phys. Lett. B **415**, 217 (1997).
8. C.J. Lister *et al.*, Abstract no. 155, in *Proceedings of the International Workshop Pingst2000* (Blums i Lund AB, 2000).
9. R. Wyss, in *NATO School Predeal, Romania* (Kluwer Academic Publishers, 2000).
10. W. Satula, R. Wyss, Nucl. Phys. A **676**, 120 (2000).
11. W. Satula, R. Wyss, Phys. Rev. Lett. **86(20)**, 4488 (2001).
12. C. Baktash *et al.*, Phys. Rev. Lett. **74(11)**, 1946 (1995).
13. F. Lerma *et al.*, Phys. Rev. Lett. **83(26)**, 5447 (1999).
14. T. Bäck *et al.*, Eur. Phys. J. A **6**, 391 (1999).
15. B. Cederwall *et al.*, Eur. Phys. J. A **6**, 251 (1999).
16. E. Ideguchi *et al.*, Phys. Lett. B **492**, 245 (2000).
17. W. Satula, R. Wyss, Phys. Scr. T **56**, 159 (1995).
18. R. Wyss, W. Satula, P. Magierski, Nucl. Phys. A **578**, 45 (1994).
19. H.C. Pradhan, Y. Nogami, J. Law, Nucl. Phys. A **201**, 357 (1973).
20. M. Górska *et al.*, Phys. Rev. Lett. **79(13)**, 2415 (1997).
21. M. Lipoglavsek *et al.*, Z. Phys. A **356**, 239 (1996).
22. M. Lipoglavsek *et al.*, Phys. Lett. B **440**, 246 (1998).
23. C. Fahlander *et al.*, Phys. Rev. C **63**, 021307(R) (2001).
24. D. Sewryniak *et al.*, Nucl. Phys. A **589**, 175 (1995).
25. D. Sohler *et al.*, to be published.